

Probabilistic Fault Displacement Hazard Analysis for North Tabriz Fault

Mohammadreza Hosseyni¹, ~~Habib¹, Habib~~ Rahimi,²

1. M.Sc. Graduated, Department of Earth Physics, Institute of Geophysics, University of Tehran, Tehran, Iran

2. Associate Professor, Department of Earth Physics, Institute of Geophysics, University of Tehran, Tehran, Iran

Corresponding author: Habib Rahimi; email: rahimih@ut.ac.ir

Abstract:

The probabilistic fault displacement hazard analysis is one of the new methods ~~in of~~ estimating the amount of ~~probabilistic possible~~ displacement in the area at the hazard of causal fault rupture. In this study, using the probabilistic approach and earthquake method introduced by (Youngs et al., 2003), the surface displacement of the North Tabriz fault has been investigated, and the ~~possible-probabilistic~~ displacement in different scenarios has been estimated. By considering the strike-slip mechanism of the North Tabriz fault and using the earthquake method, the probability of displacement due to surface ruptures caused by ~~the-the~~ 1721 and 1780 North Tabriz fault earthquakes has been explored. These events were associated with 50 and 60 km of surface rupture, respectively. The 50-60 km long section of the North Tabriz fault was selected as the source of possible surface rupture.

We considered two scenarios according to ~~probabilistic possible~~ displacements, return periods, and magnitudes ~~which are~~ reported in paleoseismic studies of the North Tabriz fault. ~~As In In~~ the first scenario, ~~probabilistic possible~~ displacement, return period, and magnitude was selected between (zero to 4.5), (645 years), and (Mw~7.7), ~~zero to 4.5; 645 years and Mw 7.7~~, respectively. In the second scenario, ~~probabilistic possible~~ displacement, return period, and magnitude ~~were was~~ selected between (zero to 7.1), (300 years), and (Mw~7.3), ~~zero to 7.1, 300 years, and Mw 7.3~~, respectively. For both mentioned scenarios, the probabilistic displacements for the ~~rate of exceedance exceedance rate~~ 5% in 50, 475, and 2475 years for the ~~probabilistic principle principle possible~~ displacements (on fault) of the North Tabriz fault have been estimated. ~~In this study, (Petersen et al., 2011) method and code have been used, and its strengths and weaknesses have been investigated. The geometry of the rupture source and parameters such as dip, depth, and rake have not been considered, which has increased uncertainty,~~

~~For the first and second scenarios, the maximum probabilistic displacement of the North Tabriz fault at a rate of 5% in 50 years is estimated to be 186 and 230 cm. Also, mentioned displacements for 5% exceedance in 475 years and 2475 years in both return periods of 645 and 300 years, are estimated at 469 and 655cm.~~

Keywords: Surface rupture, Hazard, probabilistic fault displacement, North Tabriz fault, Iran.

Field Code Changed

Commented [M1]: In the abstract section of the article, a more detailed review of the approach of the article was performed and additional contents were removed. An important point that was added in this section was to refer to following the method and code of the article (Petersen 2011). One of the major weaknesses of this article was also mentioned.

Formatted: Font: 11 pt, Complex Script Font: 11 pt

Formatted: Font: 11 pt, Complex Script Font: 11 pt

Formatted: Font: 11 pt, Complex Script Font: 11 pt

Formatted: Font: 11 pt, Complex Script Font: 11 pt

Formatted: Font: 11 pt, Complex Script Font: 11 pt

Formatted: Font: 11 pt, Complex Script Font: 11 pt

Formatted: Line spacing: 1.5 lines

Formatted: Font: 11 pt, Complex Script Font: 11 pt

Formatted: Font: 11 pt, Complex Script Font: 11 pt

Formatted: Font: 11 pt, Complex Script Font: 11 pt

Formatted: Font: 11 pt, Complex Script Font: 11 pt

Formatted: Font: (Default) Times New Roman, Complex Script Font: Times New Roman

Formatted: Font: 11 pt, Complex Script Font: 11 pt

33

34

351- **Introduction**

36 ~~Earthquakes are a serious threat to many human activities, not only because of earth-shaking but also because of~~
 37 ~~surface ruptures. Earthquakes, not only because of earth-shaking but also because of surface ruptures, are a serious~~
 38 ~~threat to many human activities.~~ Reducing earthquake losses and damages requires predicting the amplitude and
 39 location of ground movements and possible surface displacements in the future. Fault displacement hazard
 40 assessments are based on empirical relationships obtained using historical seismic rupture data. These relationships
 41 evaluate the probability of co-seismic surface slip of ruptures on fault (primary) and outside the fault (distributed) for
 42 different magnitudes and distances to the causal fault. In addition, these relationships make it possible to predict the
 43 extent of fault slip on or near the active fault ((Stephanie Baiz et al., 2019).

44 A way to reduce the effects of fault rupture hazards on a structure is to ~~develop study~~ the probability of fault
 45 displacement. This approach can ~~be taken into account~~ ~~consider~~ the rate-of-exceedance ~~rate~~ of different displacement
 46 levels of the event under ~~a structure construction , along~~ with a displacement hazard curve ((Youngs et al., 2003). ~~In~~
 47 ~~surface displacement hazard studies, non-tectonic displacements such as fault creep, aftershock, soil liquefaction, and~~
 48 ~~landslide are not considered (Petersen et al., 2011).~~ So far, fault displacement data have been collected and analyzed
 49 by several researchers to evaluate the fault rupture properties. Investigation of fault displacement and extraction of
 50 experimental relationships ~~between rupture length and magnitude, rupture length and fault mechanism, maximum~~
 51 ~~fault displacement, average fault displacement, and other cases are investigated reported~~ by Wells and Coppersmith
 52 (1993 and 1994) and reviewed by Petersen and Wesnousky (1994). ~~To be considered, Each~~ earthquake causes a
 53 superficial shaking at the site, but each earthquake does not cause a surface rupture in the area. Therefore, only the
 54 data of earthquakes that have caused the rupture in the region are used to obtain the attenuation relationships ((Youngs
 55 et al., 2003).

56 ~~A method for estimating the probabilistic fault displacement hazard for strike-slip faults in the world has been~~
 57 ~~presented and mapped due to the impact of fault displacement hazard to the fault trace type and the complexity of~~
 58 ~~this effect and hazard of fault displacement for strike-slip faults studied by (Petersen et al., 2011).~~ Principal
 59 displacements are considered primary ruptures that occur on or within a few meters of the active fault. Distributed
 60 displacements outside the fault are causative and usually appear as discontinuous ruptures or shears distance several
 61 meters to several hundred kilometers from the fault trace. The principal and distributed displacements are introduced
 62 as net displacements derived from horizontal and vertical displacements ((Petersen et al., 2011).

63 ~~To estimate the probabilistic fault displacement hazard, we used the (Petersen et al., 2011) method, but newly some~~
 64 ~~studies have been conducted in this approach. To estimate the probabilistic fault displacement hazard, we used the~~
 65 ~~Petersen et al., 2011 method, but newly some studies have been conducted in this approach. Recently, A method for~~
 66 ~~estimating the probabilistic fault displacement hazard for strike slip faults in the world has been presented, mapped~~
 67 ~~due to the impact of fault displacement hazard to the fault trace type and the complexity of this effect and hazard of~~

Formatted: No bullets or numbering

Commented [M2]: In the introduction section, by reviewing and using new articles (2020-2021), a better review of the report (literature review) was made—also a better introduction to input parameters in the study.

Formatted: Font: (Default) Times New Roman, 10 pt, Font color: Text 1, Complex Script Font: Times New Roman, 10 pt

Formatted: Indent: First line: 0"

Commented [M3]: New articles on domain (PFDHA) were briefly reviewed.

Formatted: Font color: Text 1

Formatted: Font color: Text 1

Formatted: Font color: Text 1

68 fault displacement for strike-slip faults studied (Petersen et al., 2011). Katona (2020) investigated the hazard of surface
69 displacement due to faults in the design of nuclear power plants. (Nurminen et al., (2020) concentrate on off-fault
70 rupturing and develop~~ing~~ed an original probability model for the occurrence of distributed ruptures using from 15
71 historical ~~crustal reverse~~ earthquakes. Goda (2021) proposed an alternative approach based on stochastic source
72 modeling and fault displacement analysis using Okada equations, and ~~the~~ developed method ~~is~~ was applied to the
73 1999 Hector Mine earthquake (1999).

74 Numerical values are obtained from (Petersen et al., 2011) codes, and this method has been performed in a case study
75 in northwestern Iran. In this study, several input parameters such as maximum magnitude, return period, faulting
76 mechanism, surface rupture length, Mapping Accuracy, sites located on trace, cell size, regression, and displacement
77 models, according to (Petersen et al., 2011), have been used to estimate the probabilistic displacement and exceedance
78 rate of north Tabriz fault in different scenarios.

79 The North Tabriz fault has a high level of danger by passing through the 5th district of Tabriz city, and in case of
80 possible surface rupture, it will lead to many damages in this residential area. With 150,000 people and 32,000 square
81 kilometers, this region has essential areas such as Baghmishch, Elahieh, Rashidieh town, etc. (Figure 1).

82 In this study, ~~B~~based on the results of a paleoseismic study reported by (Hesami et al. (2003) Hessami et al., 2003) on
83 the North Tabriz fault, the section with a length of 50–60 km was considered ~~as~~ a source of possible rupture in the
84 future. Sites at distances of 50 m from each other and cells with dimensions of $25 \times 25 \text{ m}^2$ on fault trace were
85 considered to estimate probability displacement. To describe the possible behavior of the displacement rupture hazard
86 of the North Tabriz fault, sites at distances of 50 m from each other and cells with dimensions of $25 \times 25 \text{ m}^2$ on fault
87 trace were considered, which is shown in Figures 1.

88 Also, according to the study ~~of by~~ by (Petersen et al., (2011), the trace of the North Tabriz fault was considered ~~as~~-a
89 simple trace due to the absence of large instrumental earthquakes ~~that are~~ associated with surface rupture. Many studies
90 have been done on the historical displacements of the North Tabriz fault. According to the ~~results of~~ paleoseismic
91 studies reported by (Hesami et al. (2003) Hessami et al., 2003) and (Ghasemi Ghassemi et al., (2015), the probabilistic
92 displacement is between (zero to 4.5) and (zero to 7.1) m, respectively. ~~The~~ magnitude and return period of large
93 earthquakes ~~are considered 645 years with~~ (Mw ~7.7 within 645 years) ~~and~~ (Mw ~7.3 within 300 years), ~~with Mw 7.3~~
94 according to (Mousavi et al., 2014) and (Dejammour Djamour et al., 2011), respectively, ~~are considered~~.

95 In ~~this study and~~ the first step, probabilistic fault displacement and ~~the~~ annual ~~rate of exceedance~~ exceedance rate of
96 displacement for two given scenarios (645 years with ~~in~~ Mw ~7.7) and (300 years with ~~in~~ Mw ~7.3) ~~have been achieved~~
97 by considering 5% ~~exceedance rate~~ in 50, 475, and 2475 years at the site with geographical coordinates (38.096,
98 46.349), ~~have been obtained~~. In the second step, due to the passage of the North Tabriz Fault through the city of Tabriz
99 ~~figure (1)~~, considering a 2 km long section from the North Tabriz Fault, the probabilistic displacement has been
100 estimated, and the probabilistic displacement 2D map is explored.

101 ~~Due to the Tabriz fault having a very high level of hazard in the future, due to the lack of instrumental data on this~~
102 ~~fault, there is increased uncertainty in the numerical calculations of this fault. The North Tabriz fault has a high level~~

- Formatted: Font color: Text 1
- Formatted: Font: 10 pt, Complex Script Font: 10 pt
- Formatted: Font color: Text 1
- Formatted: Font color: Text 1
- Formatted: Font color: Text 1
- Formatted: Font color: Text 1
- Formatted: Font color: Text 1
- Formatted: Font color: Text 1
- Formatted: Font color: Text 1
- Formatted: Font color: Text 1
- Formatted: Font color: Text 1
- Commented [M4]:
- Formatted: Font: 10 pt, Complex Script Font: 10 pt
- Formatted: Font: 10 pt, Complex Script Font: 10 pt
- Formatted: Font: 10 pt, Complex Script Font: 10 pt
- Formatted: Font: 10 pt, Complex Script Font: 10 pt
- Formatted: Font: 10 pt, Complex Script Font: 10 pt
- Formatted: Font: 10 pt, Complex Script Font: 10 pt
- Formatted: Font: 10 pt, Complex Script Font: 10 pt
- Formatted: Font: 10 pt, Complex Script Font: 10 pt
- Formatted: Font: 10 pt, Complex Script Font: 10 pt
- Formatted: Font: 10 pt, Complex Script Font: 10 pt
- Formatted: Font: 10 pt, Complex Script Font: 10 pt
- Formatted: Font color: Text 1
- Formatted: Font color: Red
- Formatted: Superscript

Commented [M5]: Due to the importance of study (PFDA) in northwestern Iran due to the level of HAZARD of possible ruptures in the future, a more in-depth explanation of the significance of this method in the case of the North Tabriz fault is done.

103 of danger by passing through the 5th district of Tabriz city, and in case of possible surface rupture, it might lead to
104 many damages in this residential area. With 150,000 people and 32,000 square kilometers, this region has essential
105 regions such as Baghmisheh, Elahieh, Rashidieh, etc. Figure (1). North Tabriz Fault, due to the devastating large
106 historical earthquakes and the possible rupture hazard of the North Tabriz Fault in the future, using the method
107 (PFDHA) is essential.

108

109 ~~2-~~ Seismotectonic

110 ~~2-~~

111 ~~3-~~ With over two million people and an area of 167 square kilometers in northwestern Iran, Tabriz is one of the
112 most populated cities in the country that has experienced devastating earthquakes throughout history. One of the
113 main problems of Tabriz City is the proximity of the city to the North Tabriz fault and the expansion of
114 constructions around it. Based on the reported historical earthquakes by Berberian and Arshadi (1979), since 858
115 AD., this city and the surrounding area have experienced several large and medium destructive earthquakes.

116 The focal mechanism of earthquakes in northwestern Iran and southeastern Turkey shows that the convergence
117 between the Saudi and Eurasian plates becomes depreciable during right-lateral strike-slip faults. The strike-slip fault
118 is the ~~southeast southeastern~~ continuation of the North Anatolian Fault into Iran, consisting of discontinuous fault
119 sections with a northwest-southeast extension (Jackson and Mackenzie et al., 1992). Some of these fault fragments
120 have been ruptured and left deformed along with the earthquakes in 1930, 1966, and 1976 (Hessami et al., 2003).

121 Nevertheless, the North Tabriz fault is one of the components of this right-lateral strike-slip system, which has not
122 had a major earthquake during the last two centuries. Among the many historical earthquakes in the Tabriz region,
123 only three devastating earthquakes with a magnitude of Ms~7.3 in 1042, 1721, and 1780 with a magnitude of Ms~7.4
124 ~~had been were~~ associated with a surface rupture along the North Tabriz fault (Hessami et al., 2003). The 1721 and
125 1780 AD earthquakes ~~were along with had~~ at least 50 and 60 km of surface rupture (about 40 km overlap), respectively.
126 (Berberian et al., 1997) believe that large earthquakes along the North Tabriz fault are concentrated at specific times
127 and spatially related.

128 The ~~(occurrence of the 1976)~~ Chaldoran earthquake in Turkey, ~~which was~~ accompanied by about 55 km of fractures,
129 indicates that the length of the surface fracture caused by ~~historic historical~~ earthquakes in this region probably varies
130 from about 50 to 60 km (Toxos et al., 1977). A more detailed study of the temporal distribution of earthquakes in
131 Tabriz by Berberian and Yates (1999) also shows the cluster distribution of earthquakes over time. Due to the absence
132 of seismic events for more than 200 years in the Tabriz area (decluttering period), the study area has passed the final
133 stages of stress storage, and it is ready to release the stored energy. Therefore, (Hessami et al., 2003) investigated
134 the Spatial-temporal concentration of earthquakes associated with the North Tabriz fault. Based on paleontological
135 seismic studies on the western part of the North Tabriz fault, (Hessami et al., 2003) introduced four earthquakes that
136 occurred continuously on ~~the part of the west the western part~~ of the North Tabriz fault. The return periods of these
137 earthquakes were suggested to be (821 ± 176) years. ~~During each seismic event of the North Tabriz fault, the amount~~

Formatted: Justified

Formatted: Font: (Default) Times New Roman, 10 pt, Font color: Text 1, Complex Script Font: Times New Roman, 10 pt

Formatted: List Paragraph, Left, Indent: Before: -0.25", Numbered + Level: 1 + Numbering Style: 1, 2, 3, ... + Start at: 1 + Alignment: Left + Aligned at: 0.25" + Indent at: 0.5"

138 of right-lateral strike-slip displacement. The amount of right-lateral strike-slip displacement, during each seismic event,
139 of the North Tabriz fault, has been estimated at (3.5 to 4.5) m. In addition, (Berberian et al., 1997) considered the
140 possibility of fracturing all parts of the North Tabriz fault at once and mentioned it as one of the critical issues in the
141 earthquake hazard for the Tabriz city and the northwestern region of Iran.

142

143

144 3-4 Methodology of probabilistic fault displacement hazard analysis

145 In this study, the method introduced by (Petersen et al., 2011) has been used to estimate the probabilistic fault
146 displacement hazard caused by the North Tabriz fault. Details of the mentioned method are provided in (Petersen et
147 al., 2011), and a summary of this approach is provided here.

148 Probabilistic seismic hazard analysis has been used since its development in the late 1960s and early 1970s to assess
149 shaking hazards and to establish seismic design parameters (Cornell, 1968 and 1971). A method for analyzing the
150 hazard of probabilistic fault displacement was introduced in two approaches of earthquake and displacement (Youngs
151 et al., 2003). This method was first proposed to estimate the displacement of Yucca Mountain faults, which were the
152 landfill of nuclear waste (Stepp et al., 2001). Then, the probabilistic fault displacement hazard analysis method was
153 introduced for an environment with normal faults, and the probability distributions obtained for each type of fault
154 in the world can be used in areas with similar tectonics (Youngs et al., 2003).

155 The earthquake approach is similar to analyzing the analysis of probabilistic seismic hazards related to displacement,
156 features such as faults, partial shear, fracture, or unbroken ground at or near the ground surface, so that the attenuation
157 relationships of the fault displacement replace the ground shaking relationships. In the displacement approach, without
158 examining the rupture mechanism, the displacement characteristics of the fault observed at the site are used to
159 determine the hazard in that area.

160 The exceedance occurrence rate of displacements and the distribution of fault displacements are obtained directly from
161 the fault characteristics of geological features (Youngs et al., 2003). To calculate the exceedance rate of
162 exceedance in the earthquake approach, similar to probabilistic seismic hazard analysis relationships were used. The
163 rate of exceedance, $v_k(z)$, is calculated according to the Cornell relationship (1968 and 1971) as follows (Youngs et
164 al., 2003):

165

$$v_k(z) = \sum_n \alpha_n (m^0) \int_{m^0}^{m_n^H} f_n(m) \int_0^\infty f_{kn}(r|m) \cdot P^*(Z > z|m, r) \cdot dr \cdot dm \quad (1)$$

166 In which the ground motion parameter Z (maximum ground acceleration, maximum response spectral acceleration)
167 exceeds the specified level (z) at the site (k). Considering Equation (1) and to calculate calculating the exceedance rate
168 of displacement (D) from a specific value (d), the displacement parameter replaces the parameters of ground motion
169 (Youngs et al., 2003):

$$v_k(d) = \sum_n \alpha_n (m^0) \int_{m^0}^{m_n^H} f_n(m) \int_0^\infty f_{kn}(r|m) \cdot P^*(D > d|m, r) \cdot dr \cdot dm \quad (2)$$

Formatted: Indent: First line: 0"

170 The expression $P(D > d | m, r)$ is the "attenuation function" of the fault displacement at or near the earth's surface. This
 171 displacement attenuation function is different from the usual ground motion attenuation function and includes the
 172 multiplication of the following two probabilities (Youngs et al., 2003):

$$P_{kn}^*(D > d | m, r) = P_{kn}(Slip | m, r) \cdot P_{kn}(D > d | m, r, slip) \quad (3)$$

173 Which D and d are the Displacements on fault (principal fault) and displacement on the outside of the fault
 174 (distributed fault), ~~respectively-respectively~~ (x, y) are considered as coordinates of the site. r, z^2, L , and s are the
 175 vertical distance from the fault, the distance of site on fault rupture to the nearest rupture, the total length of the
 176 fault surface rupture, and the rupture distance to the end of the fault, respectively. The definition of these variables is
 177 shown in figure (2).

178 The following Equation has been used to obtain the exceedance rate of probabilistic displacement due to the principal
 179 fault (on fault) (Petersen et al., 2011):

$$\lambda(D \geq D_0)xyz = \quad (4)$$

$$\alpha(m) \int_{m,s} f_{M,s}(m, s) P[SR \neq 0 | m] * \int_r P[D \neq 0 | z, sr \neq 0] * P[D \geq D_0 | L, m, D \neq 0] f_R(r) dr dmds$$

180 The magnitude of the earthquake is indicated by ~~m(m)~~ ~~-infn-relation (4-)~~, and to assess the displacement hazard due
 181 to fault rupture, ~~these probability density functions the probability density functions that~~ describe displacement
 182 potential due to earthquakes on or near a rupture, ~~as well as the probabilities that the potential for non-zero ruptures~~
 183 ~~are used~~ (Petersen et al., 2011). In the following, each of the parameters for ~~estimating estimation of~~ probabilistic fault
 184 displacement hazard is described.

185 3-1 Probability density function

186 ——— The probability density function $f_{M,s}(m, s)$ determines the magnitude of the earthquake and the location of
 187 the ruptures on a fault. Since the magnitude and the rupture position on the causal fault are correlated, a probabilistic
 188 distribution is used to calculate these parameters. In the next step, the variability in the rupture location is considered.
 189 A probability density function $f_R(r)$ is considered to define the area of perpendicular distances (r) to the site to different
 190 potential ruptures (Petersen et al., 2011).

191 3-2 Probabilities

192 ——— Probability $P[SR \neq 0 | M]$ is the ratio of cells with rupture on the principal fault to the total number of cells
 193 considered. Therefore, the probability of surface rupture $P[SR \neq 0 | M]$ is considered due to a certain magnitude M
 194 due to faulting. According to ~~studies of by~~ Wells and Coppersmith's (1993) ~~studies~~, due to ~~the formulation of~~ empirical
 195 relationships between different fault parameters, probability has been obtained for different faults in the world, such
 196 as strike-slip, normal, and revers. Therefore, in hazard analysis of fault displacement, it is necessary to investigate the
 197 possibility of surface rupture with magnitude (M) on the ground so as a result, the equation (5) introduced by Wells

198 and Coppersmith (1993) can be used. According to this relation, the coefficients a and b are constant, and strike-slip
 199 faults with -12.51 and 2.553 have been reported. This relationship has a 10% probability for the size of Mw~5 and a
 200 95% probability of surface rupture for a magnitude of Mw~7.5 ((Rizzo et al., 2011).

201

$$P[sr \neq 0|m] = \frac{e^{a+bm}}{1+e^{a+bm}} \quad (5)$$

202 This rupture probability was used to estimate the exceedance ~~displacement rate rate of displacement~~ because of
 203 earthquakes such as Loma-Prieta in 1989 with a magnitude of Mw~6.9 and Alaska in 2002 with a magnitude of
 204 Mw~6.7. These earthquakes did not cause rupture to reach the earth's surface. Therefore, these two earthquakes did
 205 not cause surface deformation and are considered non-tectonic phenomena (Petersen et al., 2011). The expression
 206 $P[D \neq 0|z, sr \neq 0]$ indicates the probability of non-zero displacement at a distance r from the rupture in an area of
 207 size z^2 and ~~due to~~ the magnitude event m associated with the surface rupture. The probability $P[D \geq D_0 | L, m, D \neq 0]$
 208 for displacements more significant than or equal to the value given at this site is intended for the principal displacement
 209 (on fault). This probability is obtained by integrating around a log-normal distribution (Petersen et al., 2011).

210

211 3-3 Rate parameter $\alpha(m)$:

212 When the potential magnitude of an earthquake ~~with~~ a certain magnitude is modeled, it is possible to estimate how
 213 often these ruptures occur. The, $\alpha(m)$, rate parameter ~~used~~ describes the frequency of repetition of these earthquakes
 214 in this model. This parameter is a function of magnitude and can only function as a single rupture function or a function
 215 of cumulative earthquakes above the magnitude of the minimum importance in engineering projects (Youngs et al.,
 216 2003). This parameter is usually based on slip rate, paleoseismic rate of large earthquakes, or historical fault rate
 217 earthquakes and is described in earthquake units per year. By removing the $\alpha(m)$ parameter from Equation (4), the
 218 Deterministic Fault Displacement Hazard can be estimated (Petersen et al., 2011).

219

220 3-4 Cell size:

221 In calculating the hazard of principal fault displacements, as shown in Eq. (4), ~~the hazard level will not change by~~
 222 ~~changing the cells' size by changing the size of the cells, the level of hazard will not change, and T~~his parameter can
 223 be examined by the availability of principal displacement data in the study area. In calculating the hazard of distributed
 224 rupture (distributed displacement), considering the method of Youngs et al. (2003), ~~the probability of surface rupture~~
 225 ~~was investigated by modeling secondary displacements up to a distance of 12 km from the fault by modeling secondary~~
 226 ~~displacements up to a distance of 12 km from the fault, the probability of surface rupture was investigated.~~ According
 227 to studies by Petersen (2011), the relationship between the calculations of the probability of rupture of the principal
 228 faults, (5), ~~in~~ calculating the probability of rupture of the distributed faults became the following relationship (Petersen
 229 et al., 2011):

230

$$\ln(p) = a(z) \ln(r) + b(z) \quad (6)$$

231 The values of the coefficients used for the cell sizes of 25×25 to 200×200 m² in the above relationship are given in
232 Table (1) (Petersen et al., 2011).

233

234 3-5 Surveying accuracy

235 ——— The accuracy of fault location is a function of geological and geomorphic conditions that play an essential
236 role in diagnosing and interpreting a geologist in converting this spatial information into geological maps and fault
237 geographic information systems. A fault map is generated using aerial photography imagery, interpretation of fault
238 patterns from geomorphology, and conversion of fault locations into a base map. In many cases, identifying the
239 location and trace of the fault may be difficult because sediments and erosion may obscure or cover the fault surface,
240 leading to more uncertainty in identifying the actual location of the fault. Therefore, trace mapped faults are divided
241 into four categories: accurate, approximate, inferred, and concealed, based on how clearly and precisely they are
242 located (Petersen et al., 2011).

243 A practical example shows that an active fault with large earthquakes repeated over several hundred years, fault
244 rupture hazard analysis should be ~~a critical topic for designing one of the critical topics considered structures or~~
245 ~~pipelines for the design of structures or pipelines that are~~ close to this fault, ~~and if this~~ the fault has a complex or
246 straightforward trace, avoiding the fault from the constructor to a distance of 150 and 300 meters, respectively. Table
247 (2-) summarizes the standard deviations for the displacements observed in strike-slip earthquakes for different
248 classifications of mapping accuracy (Petersen et al., 2011). ~~The mean displacement will be obtained according to the~~
249 ~~exponential values obtained from these fitting equations. According to the exponential values obtained from these~~
250 ~~fitting equations, the mean displacement will be obtained.~~ The following Equation has been used to obtain the mean
251 displacement (Petersen et al., 2011):

$$D_{mean} = e^{\mu + \sigma^2/2} \quad (7)$$

252

253

254 3-6 Epistemic and Aleatory uncertainty

255 There are uncertainties about the quality of mapping and the complexity of the fault trace that lead to epistemic
256 uncertainty at the site of future faults. The probability density function for r includes both epistemic and aleatory
257 components. Displacements on and off the principal fault can include ~~components of~~ epistemic uncertainty and
258 random variability. Epistemic uncertainty is related to displacement measurement errors along fault rupture. Random
259 variability is related to the natural variability in fault displacements between earthquakes. However, the measured
260 ~~rupture variability variability in ruptures~~ involves epistemic mapping uncertainties because there is currently no data
261 to separate these uncertainties. In addition, epistemic uncertainty of location is introduced due to limitations in the
262 accuracy of basic maps or images and the accuracy of the equipment used to transfer this information to the map or
263 database (Petersen et al., 2011).

264 3-7 Attenuation relationship of strike-slip faults

265 In this study, to estimate the probabilistic displacement of the North Tabriz fault, the attenuation relationship of
266 (Petersen et al., (2011) has been used. The rupture displacement data obtained from the principal fault are scattered
267 but are generally the most scattered near the fault rupture center and decrease rapidly at the end of the rupture. In some
268 earthquakes, including the Borgo Mountain earthquake in 1968, the most significant displacement was observed near
269 the end of the fault surface rupture (Petersen et al., 2011). Many ~~of the~~ collected surface rupture data behave
270 asymmetrically ruptured (Wesnousky et al., 2008).

271 However, there is currently no way to determine surface rupture areas ~~that have with~~ larger displacements. Thus, the
272 distribution of asymmetric displacements along the length of a fault will define more considerable uncertainties,
273 especially near the end of the fault rupture (Petersen et al., 2011). ~~In studying the distribution and principle~~
274 ~~displacement, two different approaches are introduced by (Petersen et al., 2011). To determine the displacement~~
275 ~~distribution, and the principal fault, two different approaches were introduced by Petersen et al. (2011).~~ In the first
276 approach, the best-fit equations using the least-squares method related to the natural logarithm of ~~magnitude and~~
277 ~~distance displacement ratio the displacement ratio of magnitude and distance~~ were developed in a multivariate analysis
278 (Paul Rizzo et al., 2013).

279 ~~In the second approach, the average displacement normalizes the displacement data as a distance function. In the~~
280 ~~second approach, the displacement data is normalized by the average displacement as a distance function. In~~
281 normalized analysis, magnitude is not directly considered but influences calculations through the presence of
282 magnitude in the mean displacement, ~~calculated through Wells and Coppersmith's studies which is calculated through~~
283 ~~the studies of Wells and Coppersmith~~ (1994). Three models (bilinear, elliptical and quadratic) were considered to
284 provide the principal fault displacement in multivariate and normalized analysis (Petersen et al., 2011).

285 However, in multivariate analysis, the three introduced models have the same aleatory uncertainty, and there is no
286 clear basis for preferring one model to ~~the~~ other models. As a result, in the probabilistic displacement hazard analysis,
287 all three models with the same weights were used according to Table (3). The results obtained from the multivariate
288 analysis were preferred ~~to over~~ the normalized analysis because, in the normalized analysis, the stochastic uncertainty
289 of calculating the mean displacement from the Wells and Coppersmith (1994) study is added to the stochastic
290 uncertainty of the results of the Petersen attenuation relationships (Paul Rizzo et al., 2013).

291
292 In this study, multivariate analysis and probabilistic displacement estimation have been used in the three mentioned
293 models. The Equation of the three models is obtained in the multivariate method as shown in Table (3), and 5%
294 uncertainty was considered in the modeling of the strike-slip displacement data (Petersen et al., 2011):
295
296

297 **4 Results and Discussions**

298 **4-1 Probabilistic displacement of north Tabriz fault**

299 ~~Assuming the mechanism of strike-slip and trace of Tabriz fault as a simple trace (due to the lack of surface ruptures~~
300 ~~of instrumental data), considering two scenarios (Mw~7.7, 645 years) and (Mw~7.3, 300 years) and a fault section~~
301 ~~with a length of 50- 60 km (as a probabilistic surface rupture in future), the probabilistic displacement, and the annual~~

Formatted: Font: 12 pt, Complex Script Font: 12 pt

Formatted: Font: 10 pt, Complex Script Font: 10 pt

302 exceedance rate is estimated by considering one of the sites located on the Tabriz fault trace related to the entire
303 segment as shown in Figure (1). Also, for each scenario, two values of displacement (zero to 4.5 m) and (zero to 7.1
304 m) were considered according to (Hessami et al., 2003) and (Ghassemi et al., 2015), respectively. Furthermore,
305 considering the reported method by (Petersen et al., 2011), the probabilistic displacements for an exceedance rate of
306 5% in 50, 475, and 2475 years for the principal probabilistic displacements (on fault) of the North Tabriz fault have
307 been explored. The obtained results in this study can be summarized as follows:

308 In the displacement (4.5 m) : maximum displacement for the first scenario (Mw~7.7, 645 years) within 5% in 50, 475,
309 and 2475 years were estimated at 186, 469, and 469 cm. For the second scenario (Mw~7.3, 300 years), the maximum
310 displacement was calculated at 230, 469, and 469 cm, respectively, as shown in figure (3a). In the displacement (7.1
311 m): maximum displacement for the first scenario of (Mw~7.7, 645 years) and 5% in 50, 475, and 2475 years was
312 estimated at 186, 655, and 655 cm. For the second scenario (Mw~7.3, 300 years), the maximum displacement was
313 calculated at 230, 655, and 655 cm, respectively, shown in figure (3b). According to the results shown in Figures (3a
314 and 3b), although the estimated maximum displacement values are equal at some distances, at farther distances
315 perpendicular to the assumed site, these numerical values are different from each other.

316 For both scenarios (Mw~7.7, 645 years and Mw~7.3, 300 years), maximum displacements for 5% in 475 years were
317 observed to a distance of 60 meters perpendicular to the assumed site. For the first scenario (Mw~7.7, 645 years),
318 maximum displacement for 5% in 2475 years using probability displacements (0 to 4.5 m) and (0 to 7.1 m) were
319 calculated up to 100m and 80m perpendicular to the assumed site, respectively. For the second scenario (Mw~7.3,
320 300 years), the maximum displacement for 5% in 2475 years using probability displacement of (0 to 4.5 m) and (0 to
321 7.1 m) were observed to (80 m) and (40 m) perpendicular to the assumed site, respectively.

322 **4-2 Comparison of different fitting models**

323 The fitting models (bilinear, elliptical, and quadratic) have similar uncertainties. In this study, the bilinear model is
324 used to obtain probabilistic displacements. In figure (4), estimated probability displacement has been compared using
325 different fitting models.

326 **4-3 Annual exceedance rate of 5% in 50years**

327 In the next step, for both (4.5 and 7.1 m) displacements, the annual exceedance rate of 5% in 50 years, at distances (64
328 and 120) m from the assumed site, has been examined and shown in figure (5). For both scenarios, (Mw~7.7, 645
329 years) and (Mw~7.7, 645 years), the results are shown in Figures (5a and 5b). In the case of displacement (4.5 m): the
330 annual exceedance rate of displacement of (D=4 m) at distances of (64 and 120) m for the first and second scenarios
331 are (1.8×10^{-4}) , (7.5×10^{-6}) , (2.16×10^{-4}) and (1.32×10^{-5}) , respectively. In the case of displacement (7.1 m): the annual
332 exceedance rate of displacement of (D=4 m) is estimated as (1.88×10^{-4}) , (7.98×10^{-6}) , (2.22×10^{-4}) , and (1.39×10^{-5}) ,
333 respectively.

334 **4-4 Probabilistic displacement of North Tabriz fault**

Formatted: Line spacing: 1.5 lines

Formatted: Font: 10 pt, Not Bold, Complex Script Font: 10 pt, Not Bold

Formatted: Line spacing: 1.5 lines

Formatted: Font: 10 pt, Not Bold, Complex Script Font: 10 pt, Not Bold

Formatted: Line spacing: 1.5 lines

Formatted: Font: 10 pt, Not Bold, Complex Script Font: 10 pt, Not Bold

Formatted: Font: (Default) +Headings CS (Times New Roman), 11 pt, Complex Script Font: +Headings CS (Times New Roman), 11 pt

Formatted: Line spacing: Multiple 1.07 li

335 In this study, we assumed the North Tabriz fault as a simple trace with the strike-slip focal mechanism. Due to the
336 lack of instrumental data on surface ruptures, two scenarios (Mw-7.7, 645years), and (Mw-7.3, 300years) was
337 considered a probabilistic surface rupture in the future. The length of the fault section was considered 50–60 km and
338 the probabilistic displacement, and the annual exceedance rate was estimated by considering one of the sites located
339 on the Tabriz fault trace related to the total segment as shown in Figure 1. In addition, for each scenario, two values
340 of displacement (zero to 4.5m) and (zero to 7.1m) were considered according to Hessami et al., 2003 and Ghassemi
341 et al., 2015, respectively. Furthermore, considering the reported method by Petersen et al., 2011, the probabilistic
342 displacements for an exceedance rate of 5% in 50, 475, and 2475 years for the principal probabilistic displacements
343 (on fault) of the North Tabriz fault have been explored. The obtained results in this study can be summarized as
344 follows:

345 By considering the reported 4.5 m probable surface displacement by Hessami et al., 2003, maximum displacement for
346 the first scenario (Mw-7.7, 645years) and 5% in 50, 475, and 2475years were estimated at 186, 469, and 469 cm. For
347 the second scenario (Mw-7.3, 300years), the maximum displacement was calculated at 230, 469, and 469cm,
348 respectively as shown in figure (3a). In addition, by considering the 7.1m probable surface displacement reported by
349 Ghassemi et al., 2015, maximum displacement for the first scenario of (Mw-7.7, 645years) and 5% in 50, 475, and
350 2475years was estimated at 186, 655, and 655cm. For the second scenario (Mw-7.3, 300years), the maximum
351 displacement was calculated at 230, 655, and 655 cm, respectively which is shown in figure (3b).

352 According to the results shown in Figures 3a and 3b, although in some cases and distances, the estimated maximum
353 displacement values are the same, at farther distances perpendicular to the site, these values are different from each
354 other.

355 For both scenarios (Mw-7.7, 645 years and Mw-7.3, 300 years), taking into account the maximum possible
356 displacements reported from other studies (0 to 4.5m and 7.1m), the maximum displacements for 5% in 475years were
357 observed up to a distance of 60 meters perpendicular to the assumed site.

358 For the first scenario (Mw-7.7, 645 years), the maximum displacement for 5% in 2475 years using probable
359 displacements 0 to 4.5m and 0 to 7.1 m were calculated up to 100m and 80m perpendicular to the assumed site,
360 respectively. For the second scenario (Mw-7.3, 300 years), the maximum displacement for 5% in 2475 years using
361 probable displacement of 0 to 4.5m and 0 to 7.1 m were observed up to 80m and 40m perpendicular to the assumed
362 site, respectively.

363 As mentioned, the fitting models (bilinear, elliptical, and quadratic) have similar uncertainties, and in this section, we
364 compared the estimated displacements obtained by using these models. In this study, the bilinear model is used to
365 obtain probabilistic displacements. The values of the probabilistic displacements were obtained for the mentioned
366 models. In figure 4, estimated probability displacement has been compared using different fitting models.

367 In the next step, for both scenarios of 4.5 and 7.1m displacements, the annual rate of exceedance of displacement (5%
368 in 50 years), at distances 64 and 120m from the assumed site, has been examined and shown in figure 5. For both
369 scenarios, Mw-7.7, 645 years and Mw-7.7, 645 years, the results are shown in Figures 5 a and b.

Formatted: Not Highlight

370 ~~Concerning~~According to passing a part of the North Tabriz fault that passes through the (15th) district of Tabriz city,
371 estimating the probabilistic displacement in this area is of great importance, and predicting the areas with a higher
372 level of surface rupture hazard is an important matter.

Formatted: Not Highlight

Formatted: Superscript

Formatted: Not Highlight

373 Considering a cross-section with a length of (2 km) from the North Tabriz fault according to Figures (6), (7), and (8),
374 the possible two-dimensional displacements for the North Tabriz fault have been estimated. ~~To estimate the~~
375 ~~probabilistic displacement, two scenarios (Mw~7.7, 645years) and (Mw~7.3, 300years) were considered. Figure (6)~~
376 ~~shows the probabilistic displacement of the two mentioned scenarios for the 5% in 50 years (by the blue color~~
377 ~~spectrum). The probabilistic displacements for the (4.5 and- 7.1 m) m-displacements for the first scenario are shown~~
378 ~~in Figures (6a) and (6b) respectively. For the second scenario, those results are shown in Figures (6c) and (6d)~~
379 ~~respectively.~~

Commented [M6]: This section examines numerical values in displacement (D=4m) for different scenarios and displacements. Numerical values are available and will be sent to you as a table if necessary.

Formatted: Font: 10 pt, Complex Script Font: 10 pt

Formatted: Font: 10 pt, Complex Script Font: 10 pt

Formatted: Font: 10 pt, Complex Script Font: 10 pt

Formatted: Not Highlight

Formatted: Not Highlight

Formatted: Not Highlight

Formatted: Not Highlight

Formatted: Not Highlight

Formatted: Font: 10 pt, Complex Script Font: 10 pt

380 For the second scenario, the probabilistic displacement values have a higher level of hazard that can be seen at greater
381 distances from the assumed sites. The probabilistic displacement of the two scenarios for the 5% in 475 and 2475
382 years are shown in Figures (7) and (8), respectively (using the blue to red color spectrum).

383 The values of displacement perpendicular to the assumed site and the amount of probability hazard in the area were
384 investigated and illustrated in Figure (9). ~~and~~The two scenarios (Mw~7.7, 645 years) and (Mw~7.3, 300 years)
385 were compared. According to Figure (9a), for 5% in 50 years: ~~the scenario (Mw~7.3, 300 years) has a higher hazard~~
386 ~~level level of hazard~~ and can be considered the worst-case scenario. The numerical value of the displacement is
387 obtained equally in the two displacement cases (4.5 and 7.1 m). The first scenario, given that it has a larger
388 magnitude than the second scenario ($\Delta m=0.4$), but due to the higher return period, has a lower hazard level level of
389 risk than the second scenario. At about 5% in 50 years as shown in Figure (9a), the second scenario has a higher level
390 of hazard than the first scenario due to the shorter return period. In the case of 5% in 475 years and 2475 years,
391 according to Figures (9b) and (9c), unlike the case of 50 years, the first scenario has a higher level of hazard and is
392 more critical and can be considered as the worst-case scenario. In the case of 5% in 475 years and 2475 years, according
393 to Figures (9b and 9c), unlike the case of 50 years, the first scenario has a higher level of hazard and is more important,
394 and can be considered as the worst-case scenario.

Formatted: Font: (Default) +Headings CS (Times New Roman), 10 pt, Complex Script Font: +Headings CS (Times New Roman), 10 pt

Formatted: Font: (Default) +Headings CS (Times New Roman), 10 pt, Complex Script Font: +Headings CS (Times New Roman), 10 pt

Formatted: Font: (Default) +Headings CS (Times New Roman), 10 pt, Complex Script Font: +Headings CS (Times New Roman), 10 pt

Formatted: Font: (Default) +Headings CS (Times New Roman), 10 pt, Complex Script Font: +Headings CS (Times New Roman), 10 pt

Formatted: Font: (Default) +Headings CS (Times New Roman), 10 pt, Complex Script Font: +Headings CS (Times New Roman), 10 pt

395 4.1 Probabilistic displacement and rate of exceedance

396 In the first step, assuming the possible surface rupture of the North Tabriz fault (50 to 60 km), displacement and the
397 annual exceedance rate are estimated by considering one of the sites located on the Tabriz fault trace related to the
398 total segment as shown in Figure 1. Considering the return periods of 645 and 300 years, the probabilistic
399 displacements of the North Tabriz fault are assumed 4.5 and 7.1 m according to Hesami et al. (2003) and Ghasemi et
400 al. (2015), respectively.

401 Given the 4.5 m probabilistic displacements reported by Hesami et al. (2003), maximum displacement for the return
402 period of 645 years at an exceedance rate of 5% for 50, 475, and 2475 years are estimated 186, 469, and 469cm,
403 respectively. The maximum displacement for a return period of 300 years is calculated at 230, 469, and 469cm. These

404 amounts of displacement were observed for the return period of 645 and 300 years at a distance of 60-100 and 60-80
405 meters from the selected site respectively, as shown in figure (3a).

406 Also, by considering the 7.1 m probabilistic displacements reported by Ghasemi et al. (2015), maximum displacement
407 for the return period of 645 years with an exceedance rate of 5% in 50, 475, and 2475 years are estimated 186, 655,
408 and 655cm, respectively. The maximum displacement for a return period of 300 years is calculated at 230, 655, and
409 655 cm. These amounts of displacement were observed for the return period of 645 and 300 years at a distance of 60-
410 80 and 40-80 meters from the selected site respectively, as shown in figure (3b).

411

412 **4-2 Comparison of different fitting models**

413 As mentioned, the fitting models (bilinear, elliptical, and quadratic) have similar uncertainties, and this section
414 compares the displacements obtained from these models. In this study, the bilinear model is used to obtain probabilistic
415 displacements. The values of the probabilistic displacements obtained for the models (bilinear, elliptical, and
416 quadratic) are shown in Figure 4.

417 **4-3 Annual exceedance rate of 5% in 50 years**

418 Assuming the trace of the North Tabriz fault and considering the bilinear model and the return period of 645 and 300
419 years, the annual rate of exceedance for the two displacement scenarios of 4.5 and 7.1m has been examined.

420 In this comparison, an annual rate of exceedance of 5% in 50 years for both displacement scenarios of 4.5 and 7.1m,
421 at distances 64 and 120m from the assumed site, has been examined in figure (5). In the case of D=4.5m, the annual
422 rate of exceedance of D=4m at distances of 64 and 120 m for 645 years is 1.81×10^{-4} and 7.51×10^{-6} and for 300 years
423 2.17×10^{-4} and 1.32×10^{-5} as shown in (6a). In the case of D=7.1m, the annual rate of exceedance of D= 4m at distances
424 of 64 and 120m for 645 years is 1.81×10^{-4} and 1.81×10^{-4} and for 300 years 1.81×10^{-4} and 1.81×10^{-4} as shown in (6b).

425

426 **4-4 Probabilistic displacement of North Tabriz fault**

427 By examining the trace of the North Tabriz fault, due to the passing from the fifth region of Tabriz city, estimating
428 the probabilistic displacement in the region is essential and predicting the areas with a higher level of hazard is an
429 important matter. Considering a 2 km long section of the North Tabriz fault according to Figures 6, 7, and 8, the two-
430 dimensional probabilistic displacements for the North Tabriz fault have been estimated. To estimate the probabilistic
431 displacement, two scenarios (Mw7.7, 645years) and (Mw7.3, 300years) were considered. Figure 6 shows the
432 probabilistic displacement of the two scenarios mentioned for the 5% exceedance rate in 50 years, by the blue color
433 spectrum. The probabilistic displacements for the 4.5 and 7.1 m displacements for the first scenario are shown in
434 Figures 6a and 6b, respectively, and for the second scenario, in Figures 6c and 6d, respectively. The probabilistic
435 displacement values for the second scenario have a higher level of hazard that can be seen at greater distances from

436 the assumed sites. The probabilistic displacement of the two scenarios for the 5% increase rate at 475 and 2475 years
437 in Figures 7 and 8, respectively, using the blue to red color spectrum is shown.

438 Due to the lack of high magnitude instrumental earthquakes and surface ruptures, the discussion about the probabilistic
439 failure level of this active fault is uncertain in the future. As a result, one of the ways to reduce the level of damage
440 and financial and human losses is to avoid construction around this fault trace due to several terrible historical
441 earthquakes.

442

443 5 Conclusion

444 Assuming the North Tabriz fault as a simple trace with a strike-slip focal mechanism, the mechanism of strike-slip and
445 trace of Tabriz fault as a simple trace, and considering two scenarios ($M_w=7.7$, 645yrs), and ($M_w=7.3$, 300yrs) and a
446 fault section with a length of 50–60 km, the probabilistic displacement of the North Tabriz fault was estimated.
447 Furthermore, considering the reported approach by Petersen (2011), the probabilistic displacements for an exceedance
448 rate of 5% in 50, 475, and 2475 years for the principal probabilistic displacements (on fault) of the North Tabriz fault
449 have been explored. The obtained results in this study can be summarized as follows. The lack of large instrumental
450 earthquakes in northwestern Iran leads to more significant epistemic uncertainty in the obtained values. Due to the
451 passing of the North Tabriz fault through Tabriz city and destructive historical earthquakes, studying methods such as
452 (PFDHA) in this area is essential to prevent disasters and economic and human losses in this region.

453 Despite following the (Petersen et al., 2011) study and code, which has been associated with favorable properties such
454 as fault mapping accuracy, and a survey of various fitting models, we mention some weaknesses here. We hope that
455 in the future, the hazard analysis community will be able to incorporate these points in future studies;

456 1. In the mentioned method, the geometry of the causal fault is not considered, so the characteristics of the source,
457 such as dip, depth, and rake, are not used, which will increase the uncertainty in calculating numerical values. The
458 North Tabriz fault has a slope to the north, so the displacement values on the north plate should be more than the
459 displacement values on the south plate.

460 2. The attenuation relationships used for this hazard analysis are also taken from a minimal database that has used
461 only 22 historical and instrumental earthquakes in the world. Surface rupture data in Asia, the United States, and other
462 parts of the world, which have different seismotectonic characteristics, cause high uncertainties in the displacement
463 and exceedance rate.

464

465 3. It is clear that probabilistic displacement values for the exceedance rate in 475 and 2475 years have similar values
466 in some cases. We can guess that one of the drawbacks of this method is the estimation of probabilistic displacement
467 values for higher exceedance rates, including (2475 years).

Commented [M7]: In the conclusion part, a better and more complete review was done, the work results were explained, and the weak and strong points of the work were mentioned

Formatted: Line spacing: 1.5 lines

Formatted: Font: 10 pt, Complex Script Font: 10 pt

Formatted: Font: 10 pt, Complex Script Font: 10 pt

Formatted: Font: 10 pt, Complex Script Font: 10 pt

Formatted: Font: 10 pt, Complex Script Font: 10 pt

Formatted: Font: 10 pt, Complex Script Font: 10 pt

Formatted: Font: 10 pt, Complex Script Font: 10 pt

Formatted: Font: 10 pt, Complex Script Font: 10 pt

Formatted: Font: 10 pt, Complex Script Font: 10 pt

Formatted: Font: 10 pt, Complex Script Font: 10 pt

Formatted: Font: 10 pt, Complex Script Font: 10 pt

Formatted: Font: 10 pt, Complex Script Font: 10 pt

Formatted: Font: 10 pt, Complex Script Font: 10 pt

Formatted: Font: 10 pt, Complex Script Font: 10 pt

Formatted: Font: 10 pt, Complex Script Font: 10 pt

Formatted: Font: 10 pt, Complex Script Font: 10 pt

Formatted: Font: 10 pt, Complex Script Font: 10 pt

Formatted: Font: 10 pt, Complex Script Font: 10 pt

Formatted: Font: (Default) +Headings CS (Times New Roman), Complex Script Font: +Headings CS (Times New Roman), (Complex) Persian (Iran)

468 4. The values obtained clearly show that the first scenario (Mw~7.7, 645 years) has a higher hazard level in high years
469 such as 475 and 2475 years because it has a higher magnitude. It is the worst case, and in 50 years, the second scenario
470 has a higher level of risk due to the shorter return period. We conclude that the return period is the most influential
471 parameter in the lower years, and in the higher years, the magnitude it is.

472 Due to the lack of high magnitude instrumental earthquakes and surface ruptures, the discussion about the probabilistic
473 failure level of this active fault is uncertain in the future. As a result, one of the ways to reduce the level of damage
474 and financial and human losses is to avoid construction around this fault trace due to several terrible historical
475 earthquakes.

476 1— We considered two scenarios according to possible displacements, return periods, and magnitudes which are
477 reported in paleoseismic studies of the North Tabriz fault.

478 2— In the first scenario, possible displacement, return period and magnitude were selected between zero to 4.5;
479 645 years and Mw~7.7, respectively. In the second scenario, possible displacement, return period and
480 magnitude were selected between zero to 7.1, 300 years, and Mw~7.3, respectively.

481 3— For both above- mentioned scenarios, the probabilistic displacements for the rate of exceedance 5% in 50,
482 475, and 2475 years for the principle possible displacements (on fault) of the North Tabriz fault have been
483 estimated. For the first and second scenarios, the maximum probabilistic displacement of the North Tabriz
484 fault at a rate of 5% in 50 years is estimated to be 186 and 230 cm.

485 4— Maximum displacements for 5% exceedance in 475 years and 2475 years in both return periods of 645 and
486 300 years are estimated at 469 and 655cm.

487 5— In this study, the probability displacement values of the North Tabriz fault have been obtained without
488 considering the dip, depth, and rake of the fault, which has caused the same displacement values in the north
489 and south plane of the fault. In future studies, it is possible to investigate the geometric properties of the
490 source producing surface rupture and reduce the recognition uncertainty in the method of probabilistic fault
491 displacement hazard analysis.

492 6— The lack of large instrumental earthquakes in northwestern Iran leads to more significant epistemic
493 uncertainty in the obtained values. Due to the passing of the North Tabriz fault through the residential area
494 of Tabriz and destructive historical earthquakes, it is crucial to estimate the possible future displacements of
495 this fault.

496

497 Conflicts of interests

498 The authors declare that they have no known competing financial interests or personal relationships that
499 could have appeared to influence the work reported in this paper.

500

501 References

502 Ambraseys, N.N., and Melville, C.P.: A History of Persian Earthquakes, Cambridge University Press, England, 236,
503 1982.

Commented [M8]: All our references were arranged (NHES standard) and rewritten in the article.

Formatted: Font: 11 pt, Complex Script Font: 11 pt

Formatted: Font: 11 pt, Complex Script Font: 11 pt

Formatted: Justified, Indent: First line: 0"

504 Barka, A.: the 17 August 1999 Izmit Earthquake, Science., 285, 5435, 1858-1859,
505 doi:10.1126/science.285.5435.1858, 1999.

506 Baize, S., Nurminen, F., Sarmiento, A., Dawson, T., Takao, M., Scotti, O., Azuma, T., Boncio, P., Champenois, J.,
507 Cinti, F.R. and Civico, R.: A worldwide and unified database of surface ruptures (SURE) for fault displacement hazard
508 analyses, Seismol. Res. Lett., 91, 499-520, https://doi.org/10.1785/0220190144, 2020.

509 Baize, S., Nurminen, F., Dawson, T., Takao, M., Azuma, T., Boncio, P., Marti, E.: A Worldwide and Unified Database
510 of Surface Ruptures (SURE) for Fault Displacement Hazard Analyses, Bull. Seismol. Soc. Am., 499-520,
511 https://doi.org/10.1785/0220190144, 2019.

512 Berberian, M. and Arshadi, S.: On the evidence of the youngest activity of the North Tabriz Fault and the seismicity
513 of Tabriz city, Geol. Surv. Iran Rep., 39, 397-418, 1976.

514 Berberian, M., & Yeats, R. S.: Patterns of historical earthquake rupture in the Iranian Plateau, Bull. Seismol. Soc.
515 Am., 89, 120-139, https://doi.org/10.1785/BSSA0890010120, 1999.

516 Berberian, M.: Seismic Sources of the Transcaucasian Historical Earthquakes, Historical and Prehistorical
517 Earthquakes in the Caucasus, 233-311, https://doi.org/10.1007/978-94-011-5464-2_13, 1997.

518 Berberian, M.: Patterns of historical earthquake rupture on the Iranian plateau. In Developments in Earth Surface
519 Processes, 17, https://doi.org/10.1016/B978-0-444-63292-0.00016-8, 2014.

520 Berberian, M., & Yeats, R. S.: Patterns of historical earthquake rupture in the Iranian Plateau, Bull. Seismol. Soc.
521 Am., 89, 1, 120-139, 1999.

522 Berberian, M.: Seismic Sources of the Transcaucasian Historical Earthquakes, Nato. Asi. 2., 233-311,
523 https://doi.org/10.1007/978-94-011-5464-2_13, 1997.

524 Berberian, M., and Arshadi, S.: On the evidence of the youngest activity of the North Tabriz Fault and the seismicity
525 of Tabriz city, Geol. Surv. Iran Rep., 39, 397-418, 1976.

526 Biasi, G. P., and Weldon, R. J.: Estimating surface rupture length and magnitude of paleoearthquakes from point
527 measurements of rupture displacement, Bull. Seismol. Soc. Am., 96, 1612-1623, 2006.

528 Bouchon, M., Bouin, M. P., Karabulut, H., Toksöz, M. N., Dietrich, M., Rosakis, A. J.: How Fast is Rupture during
529 an Earthquake? New Insights from the 1999 Turkey Earthquakes, Geophys. Res. Lett., 28, 14, 2723-2726, 2001.

530 Comfort, L.: Self-Organization in Disaster Response: The Great Hanshin Earthquake of January 17, 1995, Nat.
531 Hazards., 12, 1995.

532 Coppersmith, K. J., & Youngs, R. R.: Data needs for probabilistic fault displacement hazard analysis, J. Geodyn., 29,
533 329-343, https://doi.org/10.1016/S0264-3707(99)00047-2, 2000.

534 Cornell, B. Y. C. A.: Owing to the uncertainty in the number, sizes, and locations of future earthquakes, it is
535 appropriate that engineers express seismic risk, as design winds or floods are, in terms of return periods (Blume, 1965,
536 Newmark, 1967, Blume, Newmark and C. 58, 1583-1606, 1968.

537 Cornell, C.A., Howells, D.A., Haigh, I.P. and Taylor, C.: Probabilistic analysis of damage to structures under seismic
538 loads, Dynamic waves in civil engineering, 473-488, 1971.

539 Cornell, C. A.: Engineering seismic risk analysis, Bull. Seismol. Soc. Am., 58, 5, 1583-1606,
540 https://doi.org/10.1785/BSSA0580051583, 1968.

541 Djamour, Y., Vernant, P., Nankali, H. R., Tavakoli, F.: NW Iran-eastern Turkey present-day kinematics: Results from
542 the Iranian permanent GPS network, Earth. Planet. Sc. Lett., 307, 1-2, 27-34,
543 https://doi.org/10.1016/j.epsl.2011.04.029, 2011.

Commented [M9]: We remove all extra references

Commented [M10]: We remove all extra references

Formatted: Font: 10 pt, Complex Script Font: 10 pt

Formatted: Justified, Indent: First line: 0"

Formatted: Not Highlight

Formatted: Justified, Indent: First line: 0"

Formatted: Not Highlight

Formatted: Not Highlight

Formatted: Justified, Indent: First line: 0"

544 Djamour, Y., Vernant, P., Nankali, H. R., Tavakoli, F.: NW Iran-eastern Turkey present-day kinematics: Results from
545 the Iranian permanent GPS network, *Earth. Planet. Se. Lett.*, 307, 1–2, 27–34,
546 <https://doi.org/10.1016/j.epsl.2011.04.029>, 2011.

547 Ghassemi, M. R.: Surface ruptures of the Iranian earthquakes 1900–2014: Insights for earthquake fault rupture hazards
548 and empirical relationships, *Earth-Sci. Rev.*, 156, 1–13, <https://doi.org/10.1016/j.earscirev.2016.03.001>, 2016.

549 Goda, K.: Potential Fault Displacement Hazard Assessment Using Stochastic Source Models: A Retrospective
550 Evaluation for the 1999 Hector Mine Earthquake, *GeoHazards*, 2, 398–414,
551 <https://doi.org/10.3390/geohazards2040022>, 2021.

552 Ghassemi, M. R.: Surface ruptures of the Iranian earthquakes 1900–2014: Insights for earthquake fault rupture hazards
553 and empirical relationships, *Earth-Sci. Rev.*, 156, 1–13, <https://doi.org/10.1016/j.earscirev.2016.03.001>, 2016.

554 Hemphill-Haley, M. A., and Weldon II R. J.: Estimating prehistoric earthquake magnitude from point measurements
555 of surface rupture, *Bull. Seismol. Soc. Am.*, 89, 1264–1279, <https://doi.org/10.1785/BSSA0890051264>, 1999.

556 Hessami, K., Pantosti, D., Tabassi, H., Shabani, E., Abbassi, M. R., Fegghi, K., & Solaymani, S.: Paleoearthquakes
557 and slip rates of the North Tabriz Fault, NW Iran: Preliminary results, *Ann. Geophys-Italy.*, 46, 5, 903–916,
558 <https://doi.org/10.4401/ag-3461>, 2003.

559 Jackson, J.: Partitioning of strike-slip and convergent motion between Eurasia and Arabia in eastern Turkey and the
560 Caucasus, *J. Geophys. Res. Solid Earth.*, 97, 12471–12479, <https://doi.org/10.1029/92JB00944>, 1992.

561 Hessami, K., Pantosti, D., Tabassi, H., Shabani, E., Abbassi, M. R., Fegghi, K., & Solaymani, S.: Paleoearthquakes
562 and slip rates of the North Tabriz Fault, NW Iran: Preliminary results, *Ann. Geophys-Italy.*, 46, 5, 903–916,
563 <https://doi.org/10.4401/ag-3461>, 2003.

564 Jennings, P. C.: Engineering features of the San Fernando earthquake of February 9, 1971, California Institute of
565 Technology, (Unpublished), <https://resolver.caltech.edu/CaltechEERL:1971.EERL-71-02>, 1971.

566 Koketsu, K., Yoshida, Sh., Higashihara, H.: A fault model of the 1995 Kobe earthquake derived from the GPS data
567 on the Akashi Kaikyo Bridge and other datasets, *Earth. Planets. Sp.*, 50, 10, 803, <https://doi.org/10.1186/BF03352173>,
568 1998.

569 Lee J. C., Chu H. T., Angelier, J., Chan Y. C., Hu J. C., Lu C. Y., Rau R. J.: Geometry and structure of northern surface
570 ruptures of the 1999 Mw=7.6 Chi-Chi Taiwan earthquake: influence from inherited fold-belt structures, *J. Struct.*
571 *Geol.*, 24, 1, 173–192, [https://doi.org/10.1016/S0191-8141\(01\)00056-6](https://doi.org/10.1016/S0191-8141(01)00056-6), 2002.

572 Masson, F., Djamour, Y., Van Gorp, S., Chéry, J., Tatar, M., Tavakoli, F., Vernant, P.: Extension in NW Iran driven
573 by the motion of the South-Caspian Basin, *Earth. Planet. Se. Lett.*, 252, 1–2, 180–188,
574 <https://doi.org/10.1016/j.epsl.2006.09.038>, 2006.

575 Mirzaei, N., Gao, M. and Chen, Y. T.: Seismic source regionalization for seismic zoning of Iran: Major Seismotectonic
576 provinces, *J. Earthquake. Pred. Res.*, 7, 465–495, 1998.

577 Moss, R. E. S., & Ross, Z. E.: 2011, Probabilistic fault displacement hazard analysis for reverse faults, *Bull. Seismol.*
578 *Soc. Am.*, 101, 4, 1542–1553, <https://doi.org/10.1785/0120100248>, 2011.

579 Mousavi-Bafrouei, S. H., Mirzaei, N., and Shabani, E.: A declustered earthquake catalog for Iranian plateau, *Ann.*
580 *Geophys-Italy.*, 57, 6, <https://doi.org/10.4401/ag-6395>, 2014.

581 Nurminen, F., Boncio, P., Visini, F., Pace, B., Valentini, A., Baize, S. and Scotti, O.: Probability of occurrence and
582 displacement regression of distributed surface rupturing for reverse earthquakes, *Front. Earth Sci.*, 8, 456,
583 <https://doi.org/10.3389/feart.2020.58160>, 2020.

584 Mousavi-Bafrouei, S. H., Mirzaei, N., and Shabani, E.: A declustered earthquake catalog for Iranian plateau, *Ann.*
585 *Geophys-Italy.*, 57, 6, <https://doi.org/10.4401/ag-6395>, 2014.

Formatted: Justified, Indent: First line: 0"

Formatted: Justified, Indent: First line: 0"

Formatted: Justified, Indent: First line: 0"

Formatted: Justified, Indent: First line: 0"

586 Paul C., Rizzo Associates, I.: Probabilistic Fault Displacement Hazard Analysis Krško East and West Sites Proposed
587 Krško 2 Nuclear Power Technical Report Probabilistic Fault Displacement Hazard Analysis Krško East and West
588 Sites Proposed Krško 2 Nuclear Power Plant, Paul C Rizzo Associates, Inc., 2013.

589 Paul C., Rizzo Associates, I.: Probabilistic Fault Displacement Hazard Analysis Krško East and West Sites Proposed
590 Krško 2 Nuclear Power Technical Report Probabilistic Fault Displacement Hazard Analysis Krško East and West
591 Sites Proposed Krško 2 Nuclear Power Plant, 2013.

Formatted: Justified, Indent: First line: 0"

592 Petersen, M. D., and Wesnousky, S. G.: Fault slip rates and earthquake histories for active faults in southern California;
593 Bull. Seismol. Soc. Am., 84, 1608–1649, 1994.

594 Petersen, M. D., and Wesnousky, S. G.: Fault slip rates and earthquake histories for active faults in southern California;
595 Bull. Seismol. Soc. Am., 84, 1608–1649, <https://doi.org/10.1785/BSSA0840051608>, 1994.

Formatted: Justified, Indent: First line: 0"

596 Petersen, M. D., Dawson, T. E., Chen, R., Cao, T., Wills, C. J., Schwartz, D. P., & Frankel, A. D.: Fault displacement
597 hazard for strike-slip faults, Bull. Seismol. Soc. Am., 101(2), 805–825, <https://doi.org/10.1785/0120100035>, 2011.

598 Petersen, M. D., Dawson, T. E., Chen, R., Cao, T., Wills, C. J., Schwartz, D. P., & Frankel, A. D.: Fault displacement
599 hazard for strike-slip faults, Bull. Seismol. Soc. Am., 101, 2, 805–825, <https://doi.org/10.1785/0120100035>, 2011.

Formatted: Justified, Indent: First line: 0"

600 Ram, T. D., & Wang, G.: Probabilistic seismic hazard analysis in Nepal: Earthq. Eng. Eng. Vib., 12, 4, 577–586,
601 <https://doi.org/10.1007/s11803-013-0191-z>, 2013.

602 Rui, Ch., Petersen, M. D.: Improved Implementation of Rupture Location Uncertainty in Fault Displacement Hazard
603 Assessment, Bull. Seismol. Soc. Am., 109, 5, 2132–2137, <https://doi.org/10.1785/0120180305>, 2019.

604 Shahvar, M. P., Zare, M., and Castellaro, S.: A unified seismic catalog for the Iranian plateau (1900–2011), Seismol.
605 Res. Lett., 84, 233–249, 2013.

606 Stepp, J. C., Wong, I., Whitney, J., Quittmeyer, R., Abrahamson, N., Toro, G., Sullivan, T.: Probabilistic seismic
607 hazard analyses for ground motions and fault displacement at Yucca Mountain, Nevada, Earthquake Spectra, 17, 113–
608 151, <https://doi.org/10.1193/1.1586169>, 2001.

609 Stepp, J. C., Wong, I., Whitney, J., Quittmeyer, R., Abrahamson, N., Toro, G., Sullivan, T.: Probabilistic seismic
610 hazard analyses for ground motions and fault displacement at Yucca Mountain, Nevada: Earthq. Spectra., 17, 1, 113–
611 151, <https://doi.org/10.1193/1.1586169>, 2001.

Formatted: Justified, Indent: First line: 0"

612 Toksöz, M. N., ARPAT, E., & ŞARO&GLU, F. U. A. T.: The East Anatolian earthquake of 24 November 1976,
613 Nature., 270(5636), 423–425, <https://doi.org/10.1038/270423b0>, 1977.

614 Wells, D. L., & Coppersmith, K. J.: New Empirical Relationships among Magnitude, Rupture Length, Rupture Width,
615 Rupture Area, and Surface Displacement, Bull. Seismol. Soc. Am., 84, 974–1002,
616 <https://doi.org/10.1785/BSSA0840040974>, 1994.

617 Wells, D. L., & Coppersmith, K. J.: New Empirical Relationships among Magnitude, Rupture Length, Rupture Width,
618 Rupture Area, and Surface Displacement, Bull. Seismol. Soc. Am., 84, 4, 974–1002,
619 <https://doi.org/10.1785/BSSA0840040974>, 1994.

Formatted: Justified, Indent: First line: 0"

620 Wells, D. L., & Kulkarni, V. S.: Probabilistic fault displacement hazard analysis—Sensitivity analyses and
621 recommended practices for developing design fault displacements, NCEE 2014—10th U.S. National Conference on
622 Earthquake Engineering: Frontiers of Earthquake Engineering, October 2014, <https://doi.org/10.4231/D3599Z26K>,
623 2014.

624 Wesnousky, S. G.: Displacement and Geometrical Characteristics of Earthquake Surface Ruptures: Issues and
625 Implications for Seismic-Hazard Analysis and the Process of Earthquake Rupture, Bull. Seismol. Soc. Am., 98, 1609–
626 1632, <https://doi.org/10.1785/0120070111>, 2008.

627 Wesnousky, S. G.: Displacement and geometrical characteristics of earthquake surface ruptures: Issues and
628 implications for seismic hazard analysis and the process of earthquake rupture, *Bull. Seismol. Soc. Am.*, 98, 4, 1609–
629 1632. <https://doi.org/10.1785/0120070111>, 2008.

Formatted: Justified, Indent: First line: 0"

630 Young, C. J., Lay, T., & Lynnes, C. S.: Rupture of the 4 February 1976 Guatemalan earthquake, *Bull. Seismol. Soc.*
631 *Am.*, 79, 670-689, <https://doi.org/10.1785/BSSA0790030670>, 1989.

632 Young, C. J., Lay, T., & Lynnes, C. S.: Rupture of the 4 February 1976 Guatemalan earthquake: *Bull. Seismol. Soc.*
633 *Am.*, 79, 3, 670-689, <https://doi.org/10.1785/BSSA0790030670>, 1989.

Formatted: Justified, Indent: First line: 0"

634 Youngs, R. R., Arabasz, W. J., Anderson, R. E., Ramelli, A. R., Ake, J. P., Slemmons, D. B., Toro, G. R.: A
635 methodology for probabilistic fault displacement hazard analysis (PFDHA), *Earthquake Spectra.*, 19, 191–219,
636 <https://doi.org/10.1193/1.1542891>, 2003.

637 Youngs, R. R., Arabasz, W. J., Anderson, R. E., Ramelli, A. R., Ake, J. P., Slemmons, D. B., Toro, G. R.: A
638 methodology for probabilistic fault displacement hazard analysis (PFDHA), *Earthq. Spectra.*, 19, 1, 191–219,
639 <https://doi.org/10.1193/1.1542891>, 2003.

Formatted: Justified

640
641
642
643
644
645
646
647
648
649
650
651
652
653
654
655
656
657

658

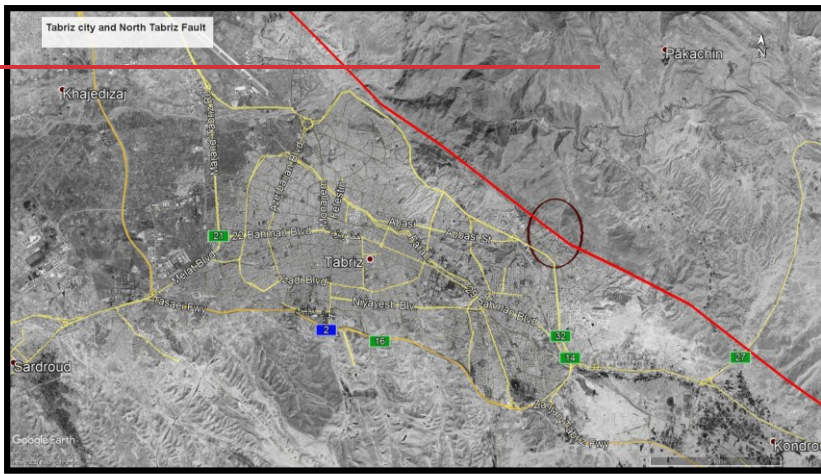
659

660

661

662

663 List of figures:



664

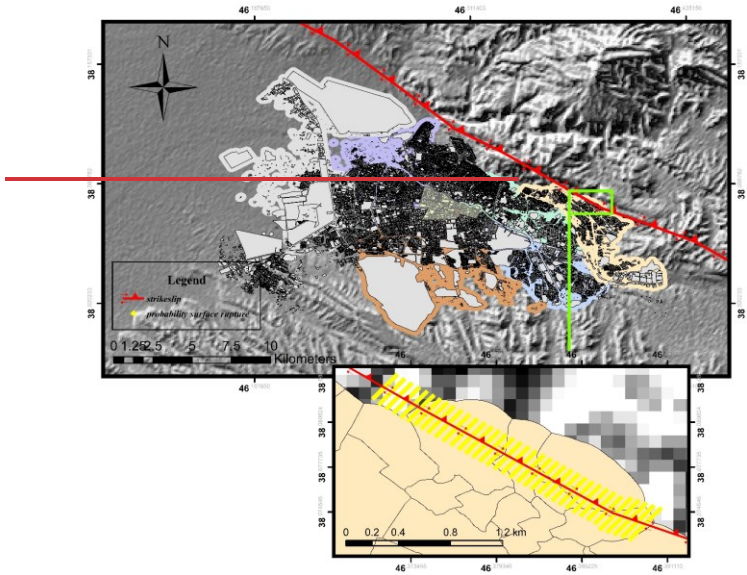
665

(a)

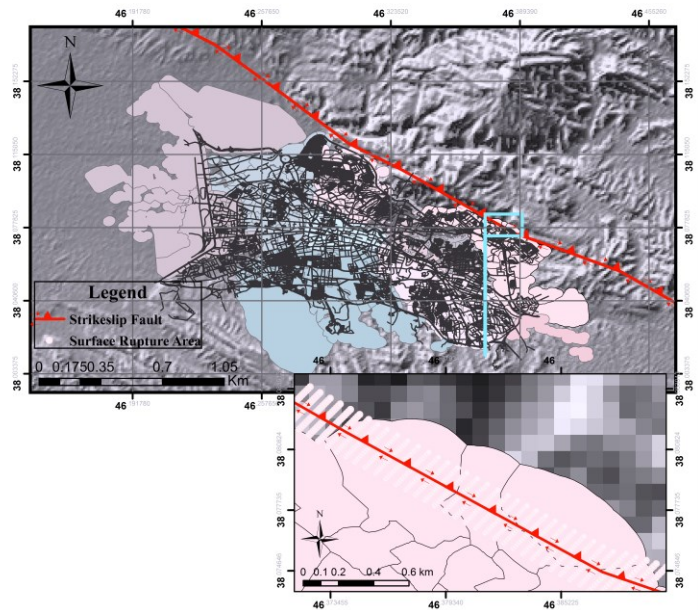
Commented [M11]: The shape (1a) was removed, and we used only the figure (1b) to show the north Tabriz fault and Tabriz city. The figure (1a) was not of good quality

Commented [M12]: figure (1) for readers with color vision deficiencies to correctly interpret, we reviewed using the Coblis – Color Blindness Simulator, and we used the (Red_Blind/tritanopia) spectrum

Formatted: Normal (Web), Justified, Indent: Hanging: 0.33", Line spacing: 1.5 lines, Tab stops: Not at 4.09"



666



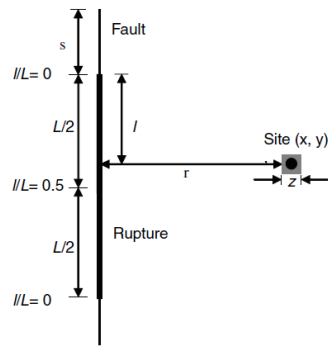
667

668

(b)

669
670
671
672

Figure (1). North Tabriz Fault and Tabriz city.
(a), Part of the North Tabriz fault considered in this study, and perpendicular profiles (b). Figure (1a and b) are generated using Google Earth with Digital Globe imagery (© Google Earth 2021).



Formatted: Centered

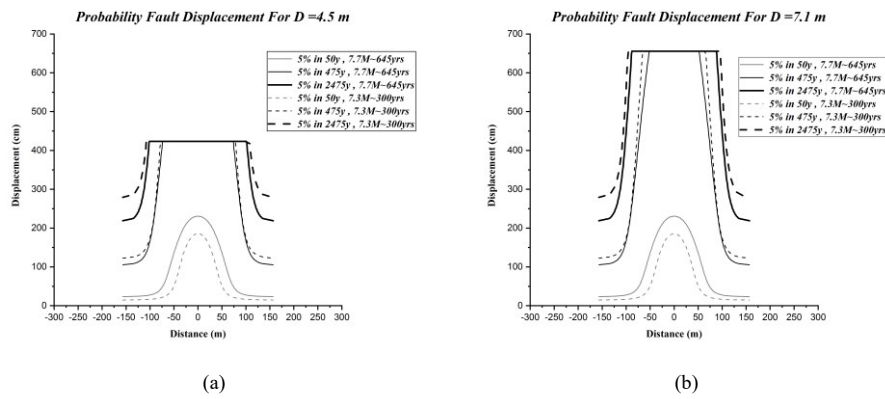
673

674
675
676
677

Figure (2). Definition of the variables used in fault rupture analysis: x and y Site coordinates, z Dimensions of the area intended to calculate the probability of fault rupture at the site (for example, dimensions of the building foundation), r: the distance from the site to the fault trace, ratio l/L : the distance from the fault so that l is the measured distance from the nearest point on the rupture to the nearest end of the rupture, L: the total length of the rupture and s: the distance from the end of the rupture to the end of the fault (Petersen et al., 2011).

678

679



680

681

Figure (3). Comparison of probability displacement, 5% exceedance rate in 50, 475, and 2475 years for a) D=4.5 m b) D=7.1 m

682

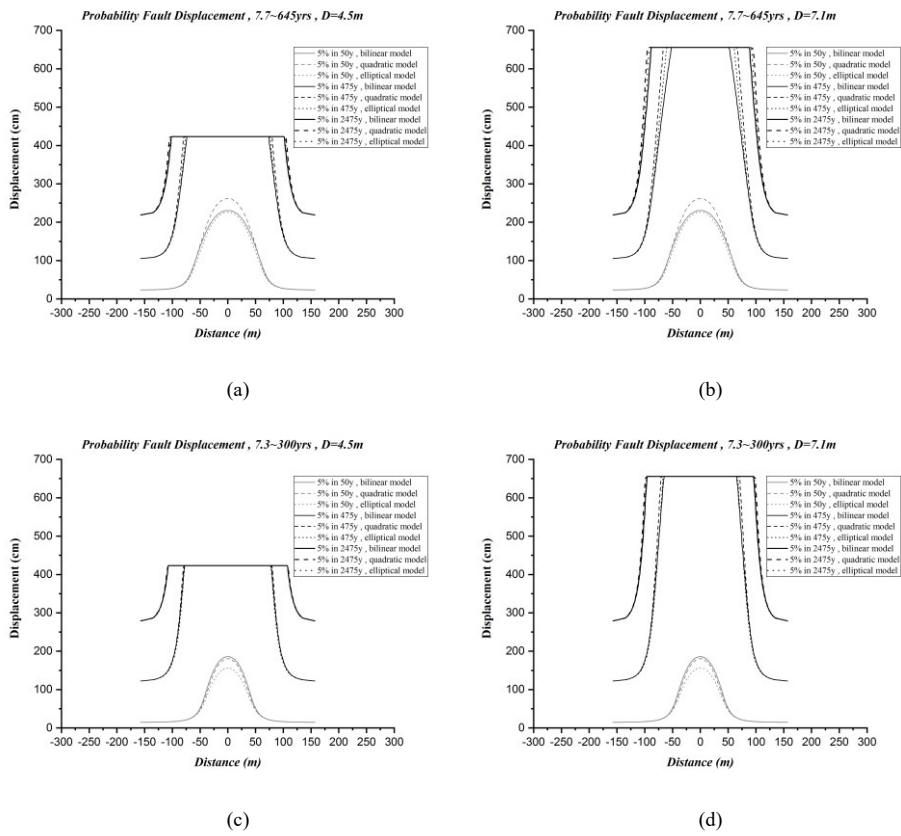
683

684

685

686

687



Formatted: Centered, Right-to-left, Indent: Before: 0.02"

688

689

Figure (4). Comparison of probability displacement, different fitting models for a) 645-year return period and D=4.5 m, b) 645-year return period and D= 7.1 m, c) 300-year return period and 4.5 m, d) return period 300- years, and D=7.1 m

690

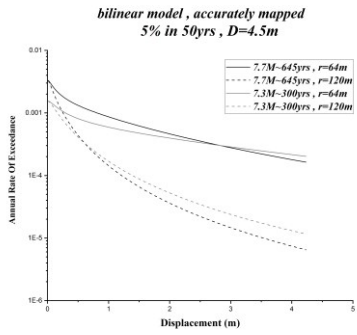
691

692

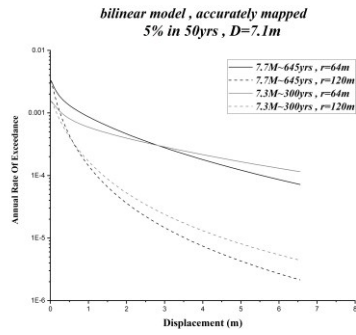
693

694

Formatted: Centered, Right-to-left, Indent: Before: 0.02"



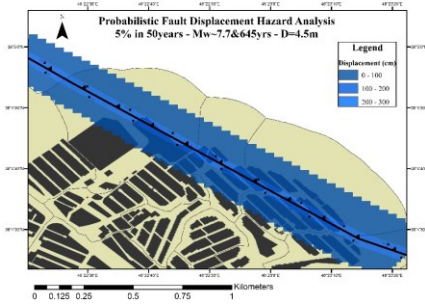
(a)



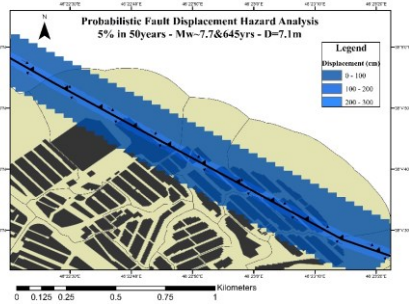
(b)

Figure (5). Comparison of the annual ~~rate of exceedance~~ ~~exceedance rate~~ of displacement for a) D=4.5 m displacement, b) D=7.1 m displacement

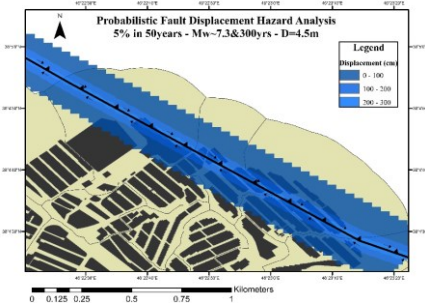
695
696
697
698
699
700
701
702
703
704
705
706
707
708
709
710
711
712
713



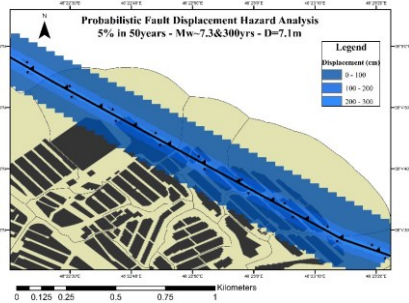
(a)



(b)



(c)



(d)

714

715 Figure (6). Probability Displacement of 5% in 50, a) Mw~7.7 and return period of 645yrs for D=4.5 m, b) Mw~7.7 and return period of 645yrs
716 for D=7.1m, c) Mw~7.3 and return period of 300yrs for D=4.5m and d) Mw~7.3 and return period of 300yrs for D=7.1m

717

718

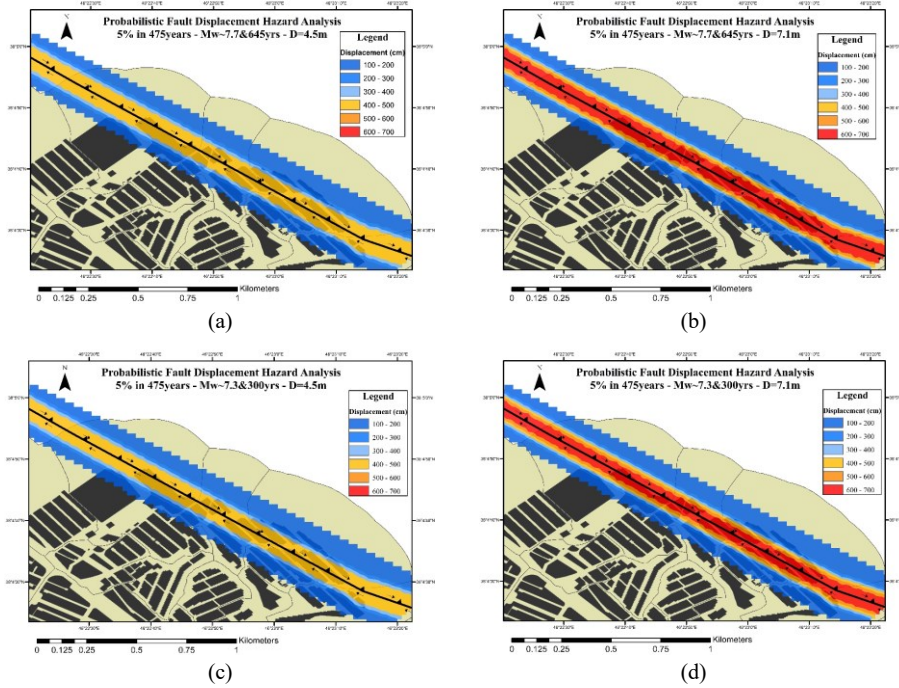
719

720

721

722

723



724

725 Figure (7). Probability Displacement of 5% in 475, a) Mw=7.7 and return period of 645yrs for D=4.5_m, b) Mw=7.7 and return period of 645yrs
 726 for D=7.1_m, c) Mw=7.3 and return period of 300yrs for D=4.5_m and d) Mw=7.3 and return period of 300yrs for D=7.1_m

727

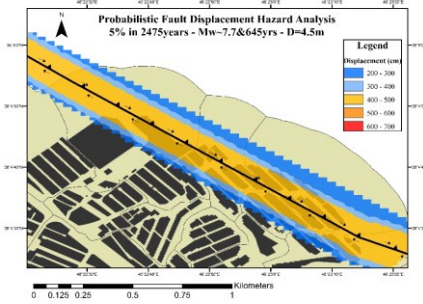
728

729

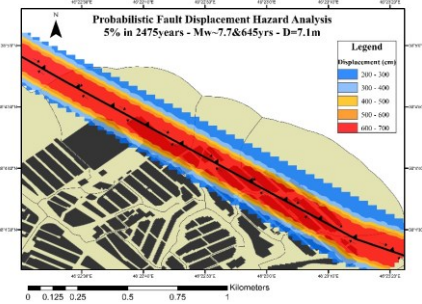
730

731

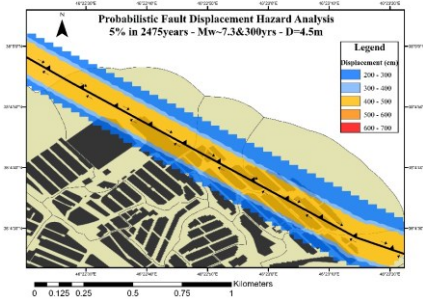
732



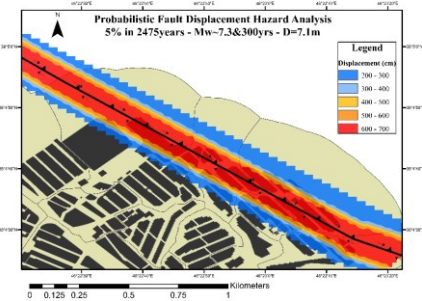
(a)



(b)



(c)



(d)

733

734 Figure (8). Probability Displacement of 5% in 2475. a) Mw~7.7 and return period of 645yrs for D=4.5 m, b) Mw~7.7 and return period of 645yrs
735 for D=7.1 m, c) Mw~7.3 and return period of 300yrs for D=4.5 m and d) Mw~7.3 and return period of 300yrs for D=7.1 m

736

737

738

739

740

741

742

743

744

745

746

747

748

749

750

751 List of Tables:

752

753 **Table 1. Probability of distributed rupture for different cell sizes (Petersen et al., 2011)**

754

755

756

757

758

759

760

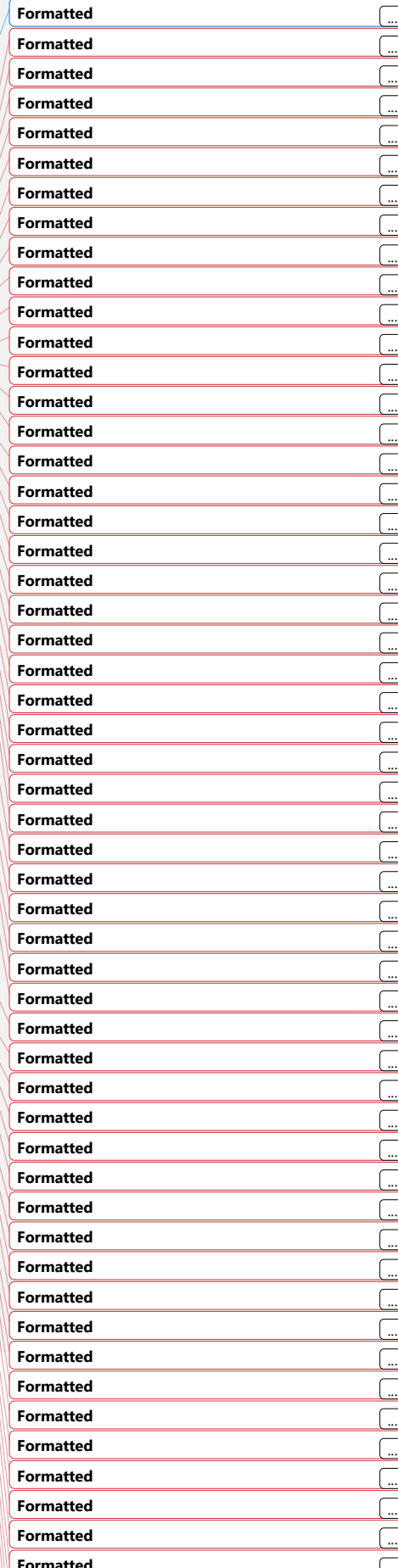
761

762

763 **Table 2. Summary of mapping accuracy: The measured distance from the mapped fault trace to the observed surface**
764 **rupture (Petersen et al., 2011)**

No.	Cell Size (m ²)	a(z)	b(z)	Standard Deviation(σ)
1	25×25	-1.1470	2.1046	1.2508
2	50×50	-0.9000	0.9866	1.1470
3	100×100	-1.0114	2.5572	1.0917
4	150×150	-1.0934	3.5526	1.0188
5	200×200	-1.1538	4.2342	1.0177

No.	Cell Size (m ²)	a(z)	b(z)	Standard Deviation(σ)
1	25×25	-1.1470	2.1046	1.2508
2	50×50	-0.9000	0.9866	1.1470
3	100×100	-1.0114	2.5572	1.0917
4	150×150	-1.0934	3.5526	1.0188
5	200×200	-1.1538	4.2342	1.0177

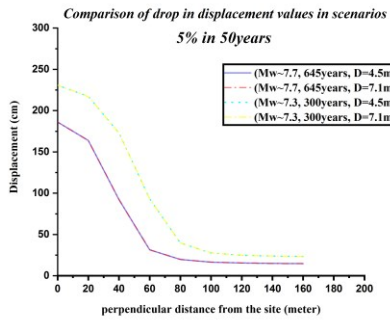


<u>Mapping Accuracy</u>	<u>Mean (m)</u>	<u>One-Sided Standard Deviation (m)</u>	<u>Two-Sided Standard Deviation on Fault (m)</u>
<u>ALL</u>	<u>30.64</u>	<u>43.14</u>	<u>52.92</u>
<u>Accurate</u>	<u>18.47</u>	<u>19.54</u>	<u>26.89</u>
<u>Approximate</u>	<u>25.15</u>	<u>35.89</u>	<u>43.82</u>
<u>Concealed</u>	<u>39.35</u>	<u>52.39</u>	<u>65.52</u>
<u>Inferred</u>	<u>45.12</u>	<u>56.99</u>	<u>72.69</u>

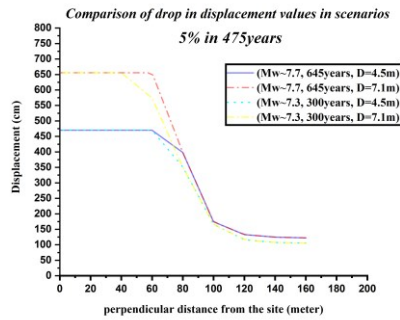
Formatted: Font: 10 pt, Complex Script Font: 10 pt

Formatted: Font: 10 pt, Complex Script Font: 10 pt

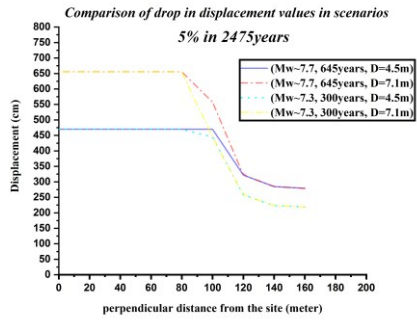
<u>Mapping Accuracy</u>	<u>Mean (m)</u>	<u>One-Sided Standard Deviation (m)</u>	<u>Two-Sided Standard Deviation on Fault (m)</u>
<u>ALL</u>	<u>30.64</u>	<u>43.14</u>	<u>52.92</u>
<u>Accurate</u>	<u>18.47</u>	<u>19.54</u>	<u>26.89</u>
<u>Approximate</u>	<u>25.15</u>	<u>35.89</u>	<u>43.82</u>
<u>Concealed</u>	<u>39.35</u>	<u>52.39</u>	<u>65.52</u>
<u>Inferred</u>	<u>45.12</u>	<u>56.99</u>	<u>72.69</u>



(a)



(b)



(c)

Figure 9. Comparison of drop in displacement values in scenarios, a) 50years, b) 475years, c) 2475years

Table 3. Different Models Used in Principal Fault Attenuation Relationships (Petersen et al., 2011)

Formatted: Left, Indent: Before: 0"

List of Tables:

Table 1. Probability of distributed rupture for different cell sizes (Petersen et al., 2011)

Formatted: Indent: Hanging: 0.33"

783
784
785
786
787
788
789
790
791
792
793
794
795
796
797
798

<u>No.</u>	<u>Cell Size (m²)</u>	<u>a(z)</u>	<u>b(z)</u>	<u>Standard Deviation(σ)</u>
<u>1</u>	<u>25×25</u>	<u>-1.1470</u>	<u>2.1046</u>	<u>1.2508</u>
<u>2</u>	<u>50×50</u>	<u>-0.9000</u>	<u>0.9866</u>	<u>1.1470</u>
<u>3</u>	<u>100×100</u>	<u>-1.0114</u>	<u>2.5572</u>	<u>1.0917</u>
<u>4</u>	<u>150×150</u>	<u>-1.0934</u>	<u>3.5526</u>	<u>1.0188</u>
<u>5</u>	<u>200×200</u>	<u>-1.1538</u>	<u>4.2342</u>	<u>1.0177</u>

Formatted: Left

Table 2. Summary of mapping accuracy: The measured distance from the mapped fault trace to the observed surface rupture (Petersen et al., 2011)

<u>Mapping Accuracy</u>	<u>Mean (m)</u>	<u>One-Sided Standard Deviation (m)</u>	<u>Two-Sided Standard Deviation on Fault (m)</u>
<u>ALL</u>	<u>30.64</u>	<u>43.14</u>	<u>52.92</u>
<u>Accurate</u>	<u>18.47</u>	<u>19.54</u>	<u>26.89</u>
<u>Approximate</u>	<u>25.15</u>	<u>35.89</u>	<u>43.82</u>
<u>Concealed</u>	<u>39.35</u>	<u>52.39</u>	<u>65.52</u>
<u>Inferred</u>	<u>45.12</u>	<u>56.99</u>	<u>72.69</u>

Formatted: Left

799
800
801
802
803
804
805
806
807
808
809
810
811
812
813
814
815
816
817
818
819
820
821
822

823

Table 3. Different Models Used in Principal Fault Attenuation Relationships (Petersen et al., 2011)

<u>Analysis Type</u>	<u>Model</u>	<u>Weight</u>
<u>Multivariate</u>	<u>BILINEAR</u> $\ln(D)=1.7969Mw+8.5206(l/L)-10.2855, \sigma_{in} = 1.2906, l/L \leq 0.3$ $\ln(D)=1.7658Mw-7.8962, \sigma_{in} = 0.9624, l/L \geq 0.3$	<u>0.34</u>
	<u>QUADRATIC</u> $\ln(D)=1.7895Mw+14.4696(l/L)-20.1723(l/L)^2-10.54512, \sigma_{in} = 1.1346$	<u>0.33</u>
	<u>ELLIPTICAL</u> $\ln(D)=3.3041\sqrt{1 - \frac{1}{0.5^2}[(l/L) - 0.5]^2}+1.7927Mw-11.2192, \sigma_{in} = 1.1348$	<u>0.33</u>

824

825

826

827

828

829

830

831

832

833

834

835

836

837

|838

839